CHANDRA
X-ray Center   60 Garden St., Cambridge Massachusetts 02138 USA

1   Optical Axis, Focal Point and Aimpoint

The positions of the Optical Axis, Focal Point and Aimpoint are critical for the optimal operation of the Chandra X-ray Observatory. They are defined as follows:

- Optical Axis: In an optical system, the optical axis is an imaginary line that defines the path along which light propagates through the system. It is often coincide with the axis of symmetry of the system surfaces. In this Memorandum, we define it as the following, which has the same meaning as the above definition: Optical Axis is the axis perpendicular to the focal plane at the Focal Point.

- Focal Point: Point on the focal plane where the sharpest PSF is located.

- Aimpoint: Point on the focal plane where the image of a source with zero Y and Z offsets is located.

For ideal Wolter-I X-ray Mirrors:

- The optical axis is the axis of symmetry of both paraboloid and hyperboloid mirror surfaces; and it passes through both Focal Point and Aimpoint (i.e. Focal Point and Aimpoint are the same point).

For the actual Chandra Telescope Mirror Assembly – HRMA:

- The Focal Point and the Aimpoint were not at the same point after the Chandra launch, and they have been drifting since.

- The positions of the Optical Axis, Focal Point and Aimpoint have been monitored continuously since the Chandra launch.

- The Focal Point position can be affected by the distortion of the HRMA and the relative position change between the HRMA and the detectors, which includes, but not limit to: the shift of the SIM, the drift of detectors relative to the SIM, the bending the the optical bench, etc.

- The Aimpoint position can be affected by, but not limit to: the relative position change between the aspect system and the optical bench, in addition to all the factors that can affect the Focal Point position.

- The initial (nominal) Optical Axis was determined from the raster scan measurements made with HRC-I in September 1999 (Maxim Markevitch: http://cxc.harvard.edu/cal/Hrma/optaxis/fine_opax_newconv.html).

- The nominal Aimpoint was determined from the absolute pointing measurements made with ACIS-S from September 1999 to April 2000 (Tom Aldcroft: http://cxc.harvard.edu/mta/ASPECT/abs_point.html).

- Based on the above measurements, the Focal Point and Aimpoint were separated by $\sim 18.6''$.

- Where have they been since then? – the motivation of this study.

2 On-orbit calibration of the Optical Axis

The HRC-I and HRC-S gain maps were calibrated by using raster scans of Y and Z offset with bright point sources (HR 1099 and Ar Lac). These calibration data are used to determine the position of the Chandra Optical Axis. Tables 1 and 2 show the calibration made until September 2005. All the raster scans were centered at the centers of HRC-I or HRC-S, except the first measurement made with the HRC-I immediately after launch on Sept. 2, 1999, which was centered near the upper corner of the HRC-I. All the raster scans were made with source Ar Lac, except the first one, which was made with HR1099.

Figure 1 shows the layout of the Chandra Science Instrument Module (SIM) with the four detectors and their SIM-Z offset. The SIM can only be moved in Z direction.

Table 1: Raster Scan with HRC-I

Date	Source	Sim-Z
1999-09-02	HR 1099	91.8655 mm
1999-10-03	Ar Lac	126.9855 mm
1999-12-09	Ar Lac	126.9855 mm
2000-12-12	Ar Lac	126.9855 mm
2002-01-26	Ar Lac	126.9855 mm
2003-02-22	Ar Lac	126.9855 mm
2004-11-25	Ar Lac	126.9855 mm
2005-09-27	Ar Lac	126.9830 mm

Table 2: Raster Scan with HRC-S

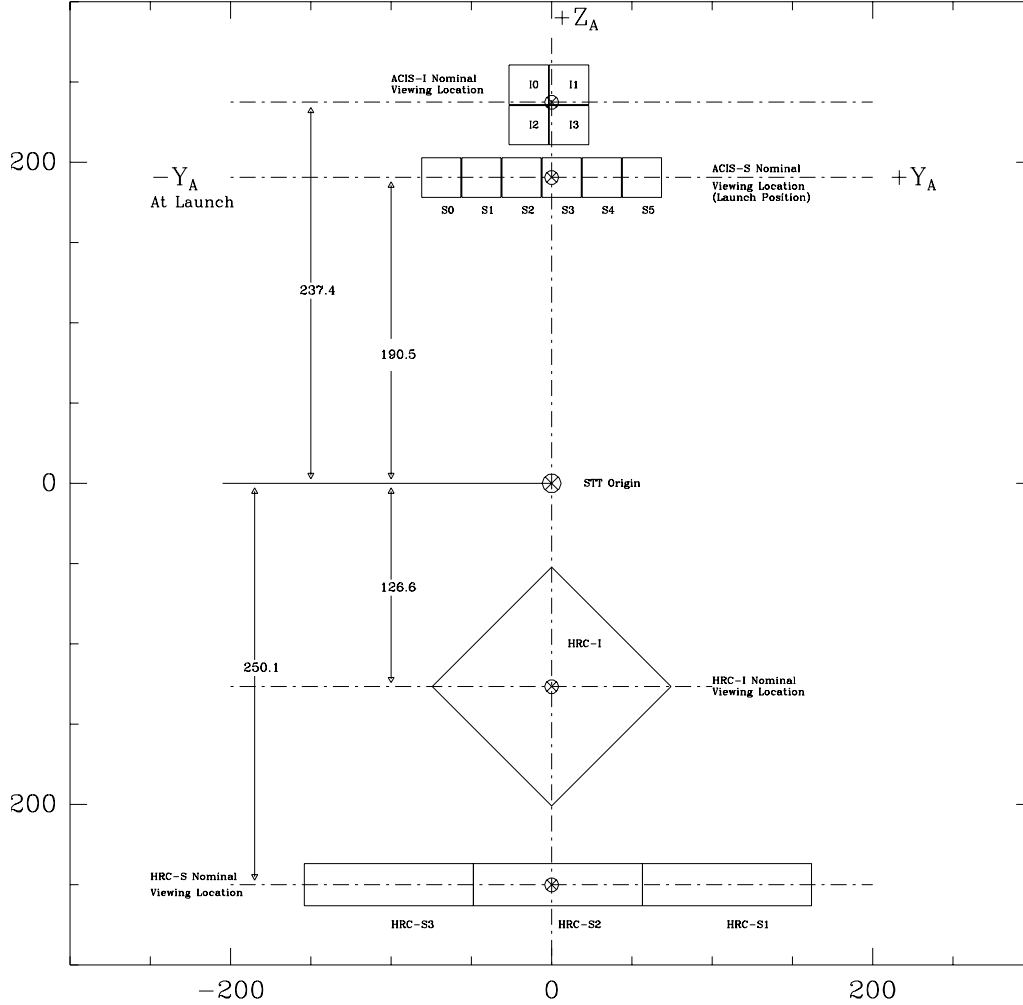| Date	Source	Sim-Z
2000-12-20	Ar Lac	250.4660 mm
2001-05-14	Ar Lac	250.4660 mm
2002-01-26	Ar Lac	250.4660 mm
2002-08-09	Ar Lac	250.4660 mm
2003-02-22	Ar Lac	250.4660 mm
2003-09-01	Ar Lac	250.4660 mm
2004-02-09	Ar Lac	250.4660 mm
2004-11-28	Ar Lac	250.4660 mm
2005-02-10	Ar Lac	250.4660 mm
2005-09-01	Ar Lac	250.4660 mm

Figure 1: The Chandra SIM Translation Table, showing the flight focal plane instrument to scale. Distance in mm. Coordinate system is AXAF-STT-1.0.

3 Data Analysis

3.1 Data

Chandra is dithered during all observations in a Lissajous figure. For observations with the HRC , the dither amplitude is 40 arcsec peak-to-peak, with nominal periods of 1087 (in Y) and 768 (in Z) seconds (POG Rev.8, p129). Figures 2 and 3 show two pointings of the raster scan data (ObsID: 1385 and 4294), in SKY (dither is removed) and CHIP (dither is shown) coordinates. ObsID 1385 has 19ks exposure time. So its image in CHIP coordinates covers the entire dither region. ObsID 4294 and most of the raster scan data pointings have only 1ks exposure time. So its image in CHIP coordinates, as well as in DET and TDET coordinates, only covers part of the dither pattern.

3.2 Determine the Center

The center of each image is determined in an iterative fashion. The image is rebinned onto a very coarse grid, and the brightest bin is used as the initial center. This works well for images with a single point source (which these are), because it relies almost exclusively upon the source events and is not greatly influenced by background events. A more precise center is then determined from the first moment of the events within a fixed circular aperture centered on the initial center.

This new center is used as the starting point for the iterative scheme. The standard deviation of the distance of all of the events from the center is calculated, and the first moment of the events within a circular aperture with a radius of a given multiple of the standard deviation is calculated. If this latest center is the same as the last (within set tolerances), the process is halted, otherwise the iterations continue until either the tolerance is met or a set number of iterations has been reached.

The error of the center is $\sigma = \sqrt{\Sigma r_i^2 / N}$, where i=1,...,N; N is the number of events in the image. r_i is the distance of the event i to the center.

3.3 Analysis Procedure

The data analysis is carried out in following steps:

1. For each image, the center and its σ in SKY coordinates are calculated using all the events.

2. Each image is cut into two smaller images: one by an 1-σ circular aperture and and by a 5-σ circular aperture. These two images with the scattered and background events removed are used in the subsequent data analysis.

3. In order to estimate the errors, resampling method (with replacement) is applied. For each cut images with N events, randomly pick events M times from the pool. After each pick, the event is put back into the pool, so it may be picked again later. Here we let M=N. So the resampled image still have N events. But it is different from the original image, because some of the events have been picked more than once and some events were never picked.

4. The center of each resampled 1-σ cut image in CHIP coordinate is calculated. Because the 1-σ cut was done in the SKY coordinate, the 1-σ cut image in CHIP coordinate is essentially a 2-σ wide band centered around the dither trace. Notice that the center calculated this way is not necessarily the center of the Lissajous dither pattern (i.e. the aimpoint of the pointing). To calculate the optical axis, we need to use this center, not the dither center, in order to obtain the weighted CHIP positions corresponding to their encircled energy. 1000 resampled images are treated this way. The average position (in CHIPX and CHIPY) and their standard deviation are assigned to be the position and error for the given raster scan pointing in the CHIP coordinate.

5. The Encircled Energy (EE) radii (10% − 99%) of each resampled 5-σ cut image is calculated, around the center in the SKY coordinate. Errors of EE were calculated using the resampling method as described above.

6. The EE radii (r) in SKY coordinate vs. the center (x,y) in CHIP coordinate are fit to a quadratic function:

$$r_{EE_i}(x,y) = c_0 + c_1 x + c_2 y + c_{11} x^2 + c_{12} xy + c_{22} y^2 \tag{1}$$
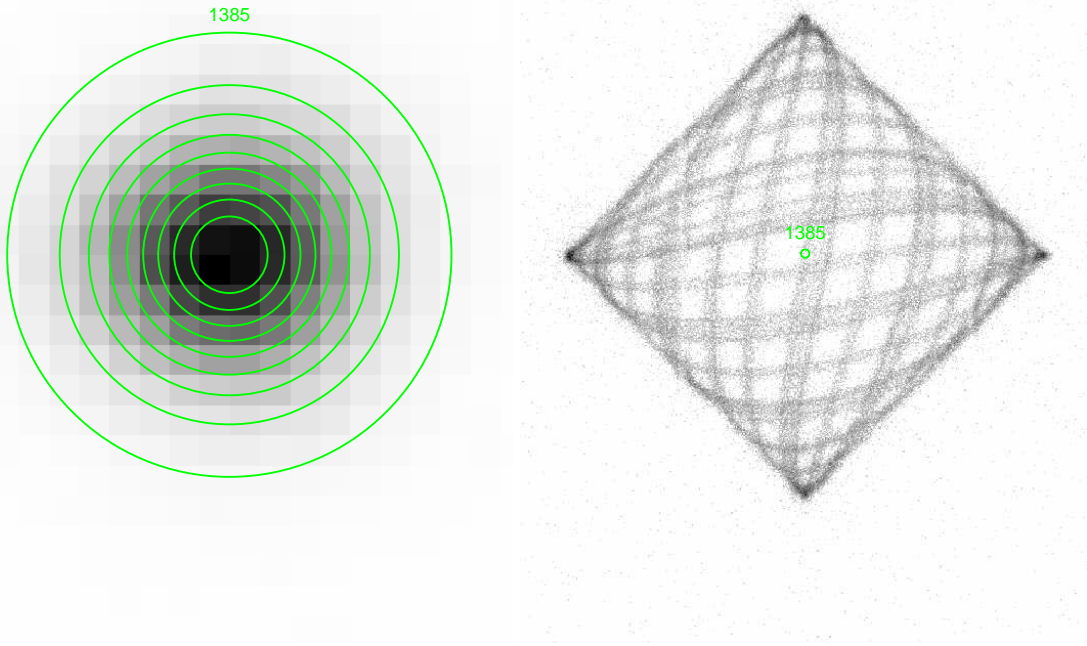
where $i = 10\% - 99\%$.

Figure 2: HRC-I observation of Ar Lac with 19ks exposure time and zero Y and Z offsets (obsid 1385). Left: image in SKY coordinates with 10% – 90% encircled energy circle overlay. Right: image in CHIP coordinates with the calculated center marked. This calculated center is at the center of the Lissajous dither pattern.

7. By definition, optical axis for each fit is at $(x_0, y_0)_i$ where r_{EE_i} reaches minimum. The final optical axis (x_0, y_0) is the weighted (by their x_0 and y_0 errors) mean of $i = 50\%, 60\%, 70\%, 80\%, 90\%$. Larger or smaller i's tend to have greater errors.

8. Aimpoint positions were calculated for each set of raster scan, using the script - "aspcal" - provided by Jonathan McDowell. This script uses the ASPECT data to calculate the Aimpoint position for any given obsid.

Figure 4 is the first HRC-I raster scan observation taken on 1999-09-02. There is likely an error of the CHIP position of the ObsID 1120. It is supposed to be at the center of the scan pattern. But this point has negligible effect on the determined optical axis. Figure 5 is the latest HRC-I raster scan observation taken on 2005-09-27. All the HRC-I raster scans except the first were taken in this pattern. Figure 6 is the latest HRC-S raster scan observation taken on 2005-09-01. All the HRC-S raster scans were taken in this pattern.

Figure 7 shows the quadratic fit of HRC-I raster scan data from 2005-09-27. Figure 8 is a zoomed in view of Figure 5, which shows the Optical Axis and Aimpoint positions.
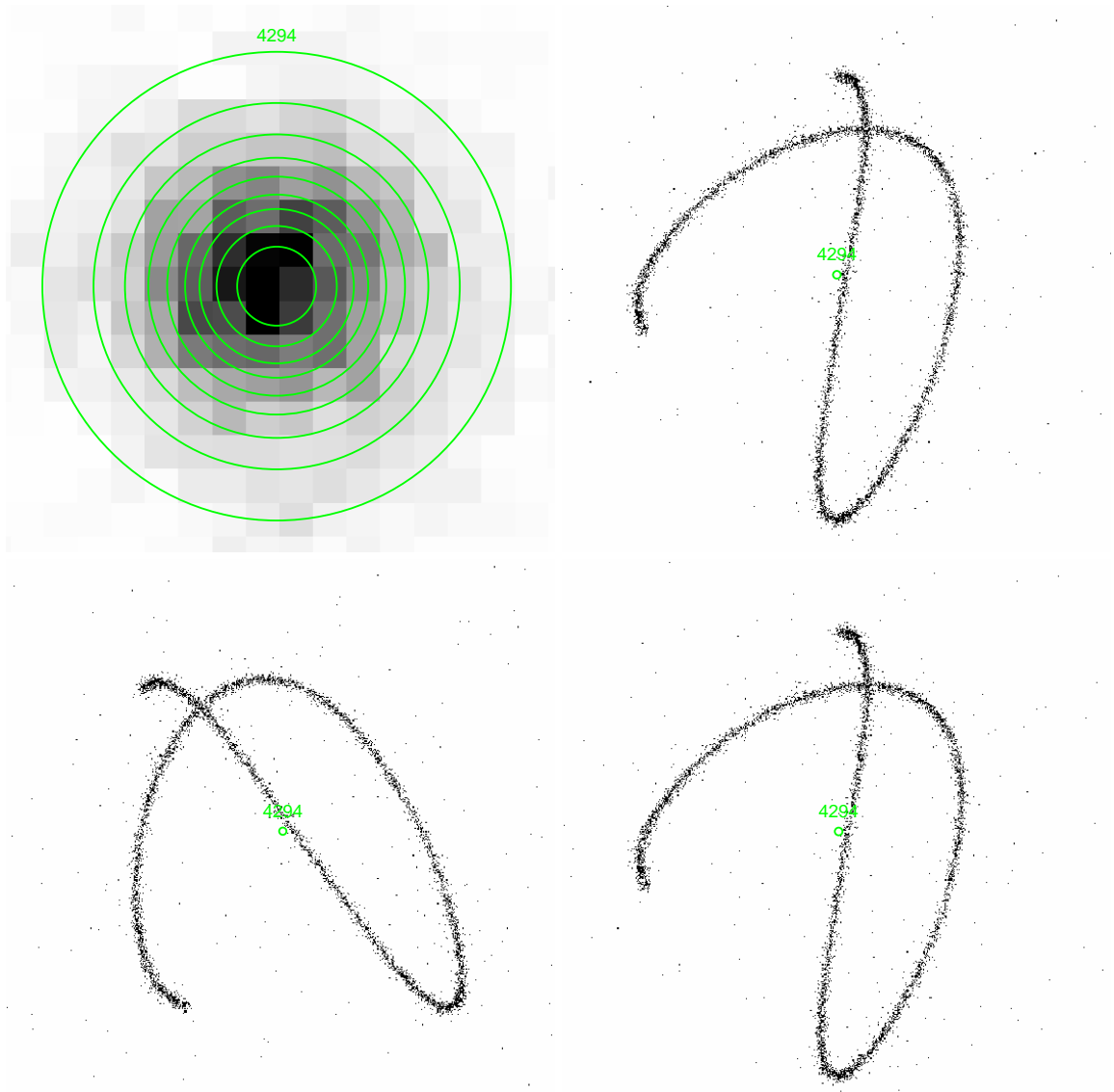
Figure 3: HRC-I observation of Ar Lac with 1ks exposure time and zero Y and Z offsets (obsid 4294). UL: image in SKY coordinates with 10% – 90% encircled energy circle overlay; UR: image in CHIP coordinates with the calculated center marked; LL: image in DET coordinates with the calculated center marked; LR: image in TDET coordinates with the calculated center marked.
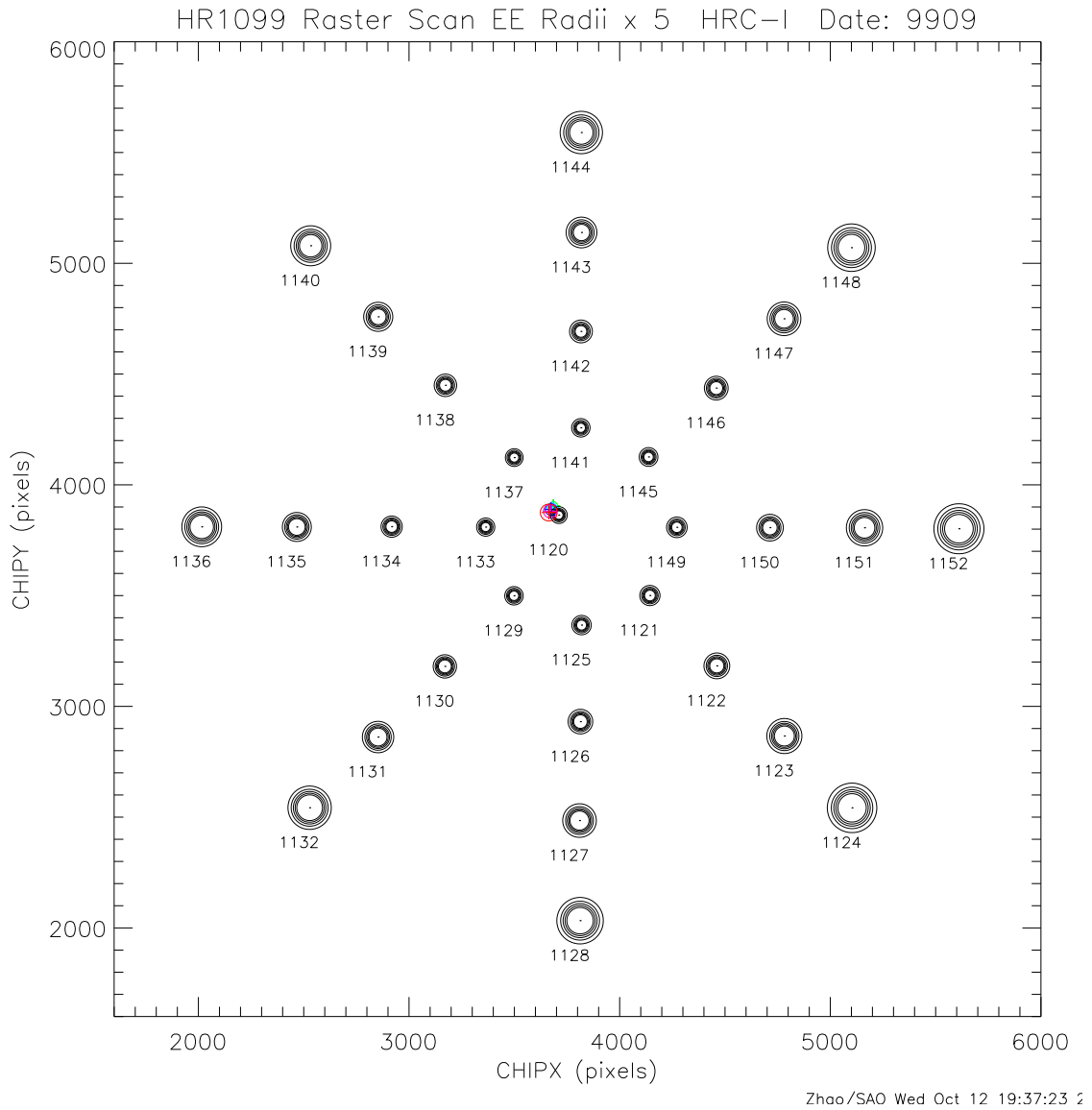
Figure 4: HRC-I raster scan observation of HR 1099 with 1ks exposure time for each scan point (Date: 1999-09-02). Circles around each observation point are the 50% − 90% EE circles × 5.

Figure 5: HRC-I raster scan observation of Ar Lac with 1ks exposure time for each scan point (Date: 2005-09-27). Circles around each observation point are the 50% – 90% EE circles × 5.
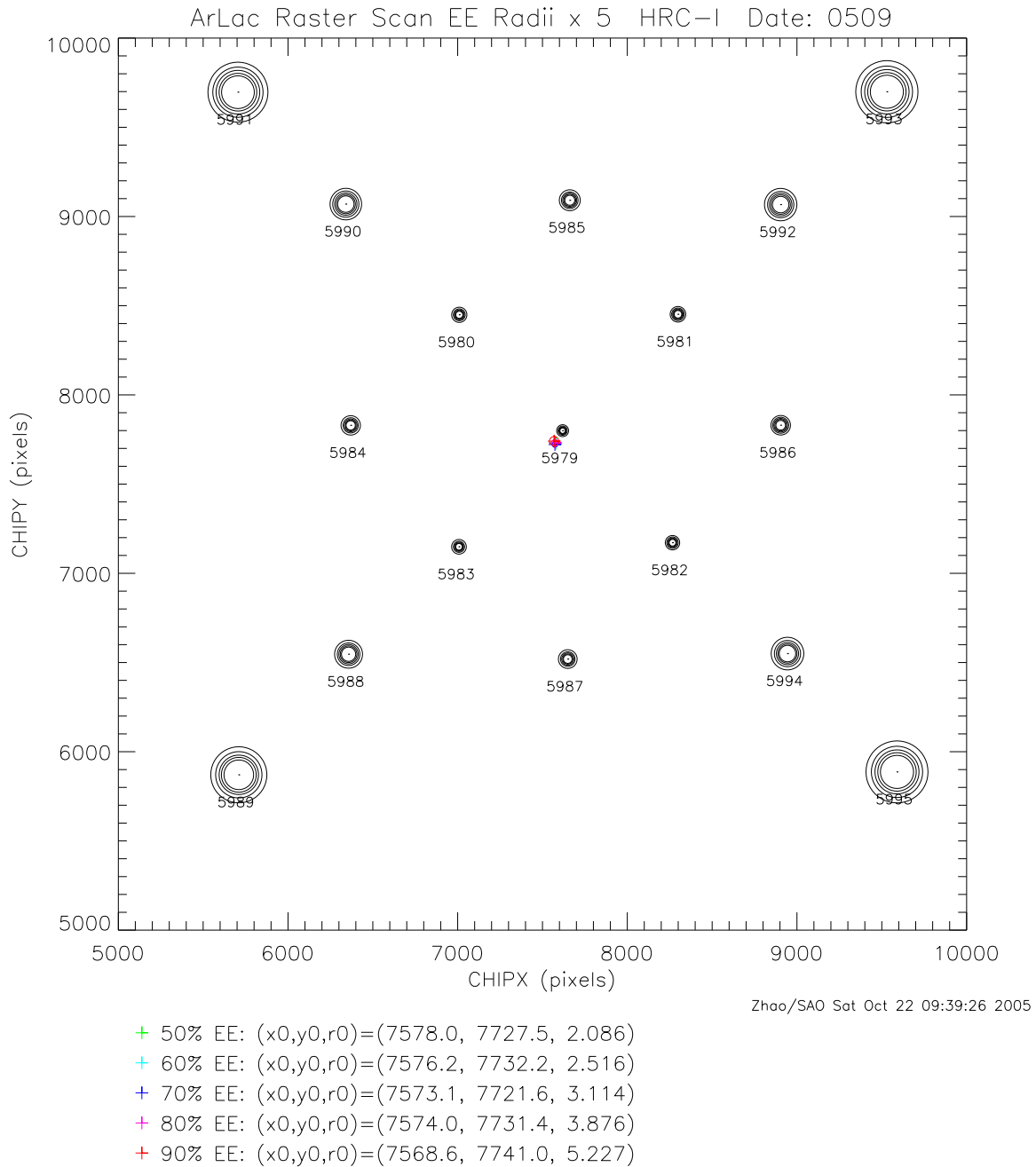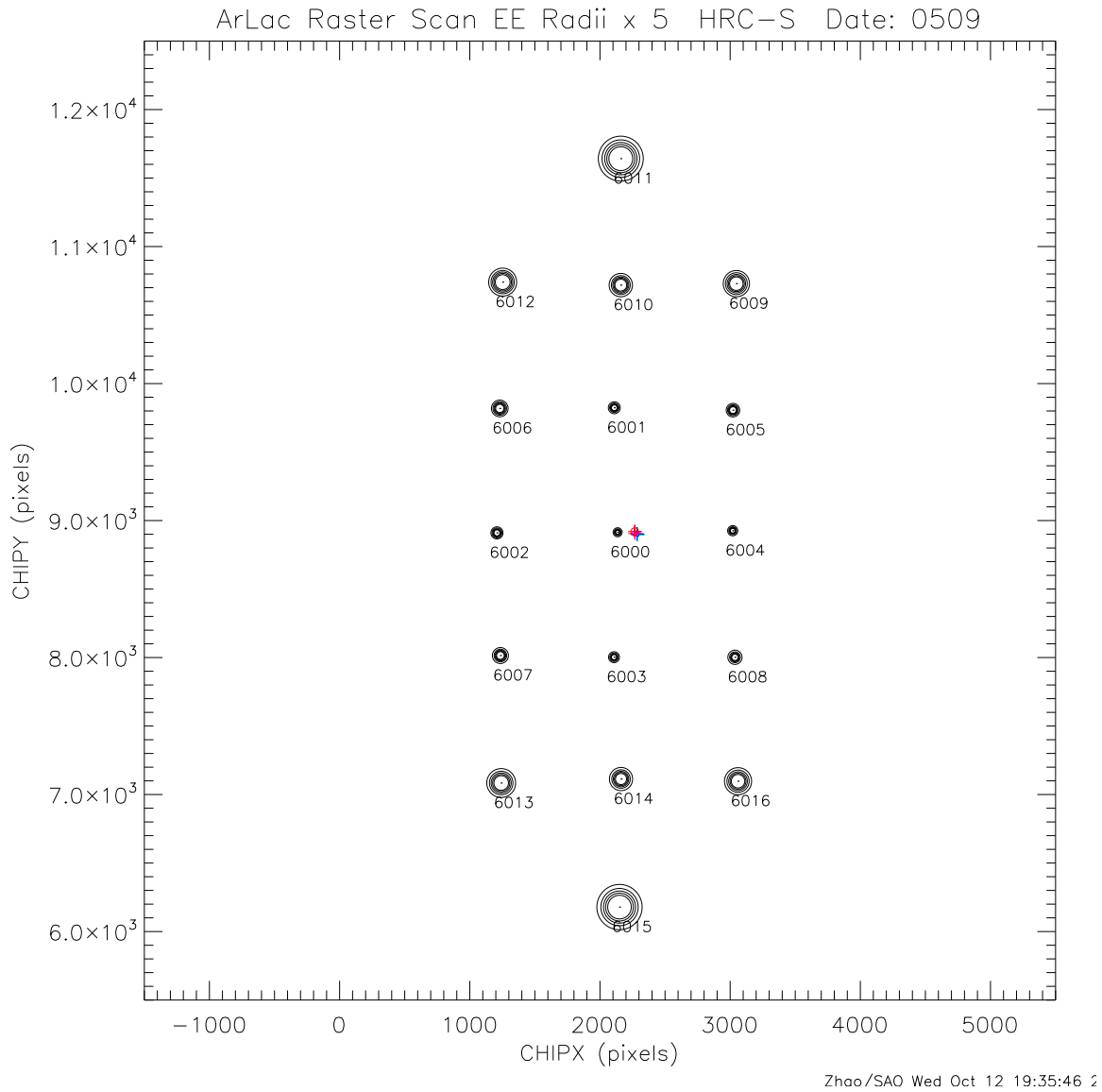
Figure 6: HRC-S raster scan observation of Ar Lac with 1ks exposure time for each scan point (Date: 2005-09-01). Circles around each observation point are the $50\% - 90\%$ EE circles $\times$ 5.
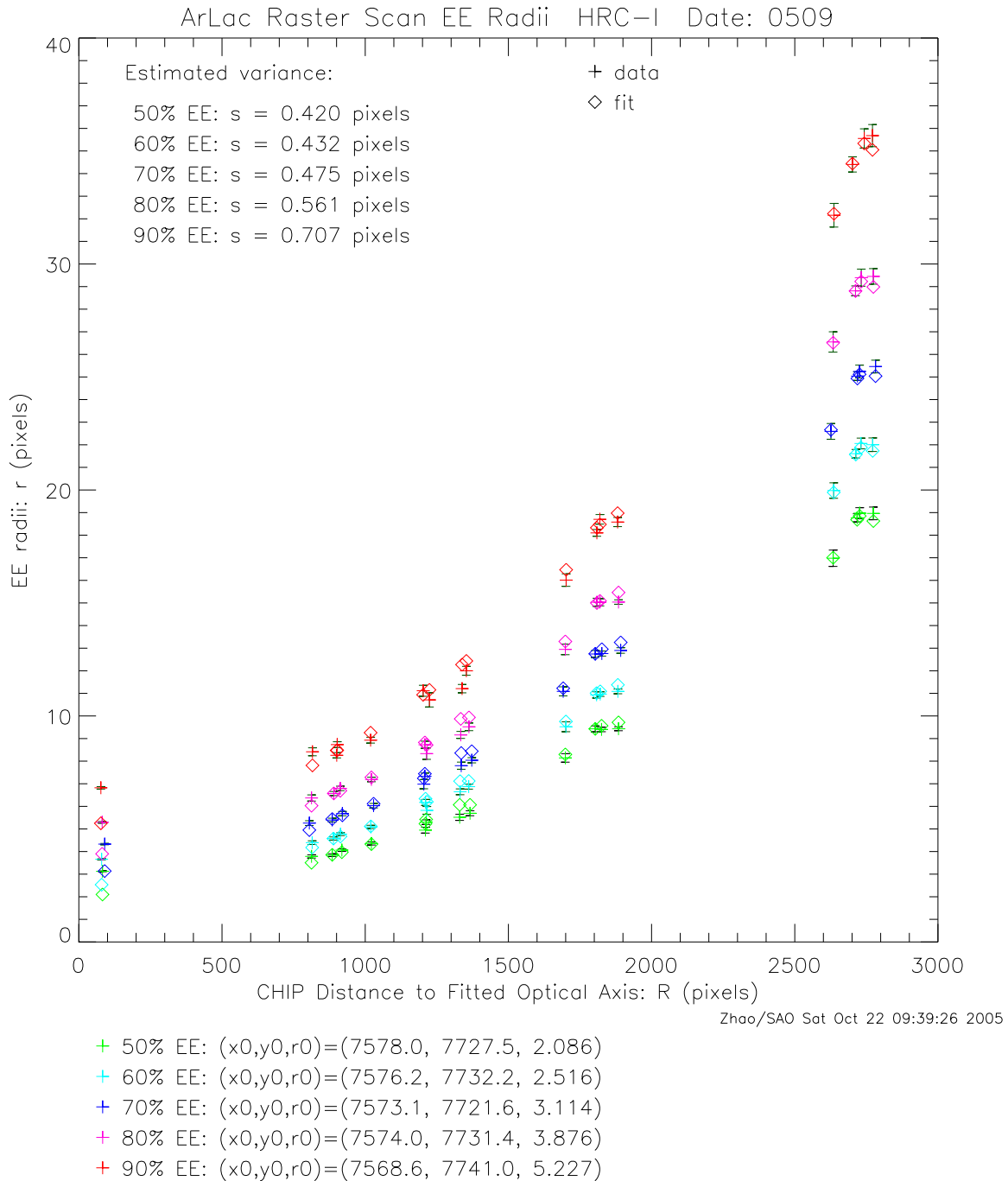
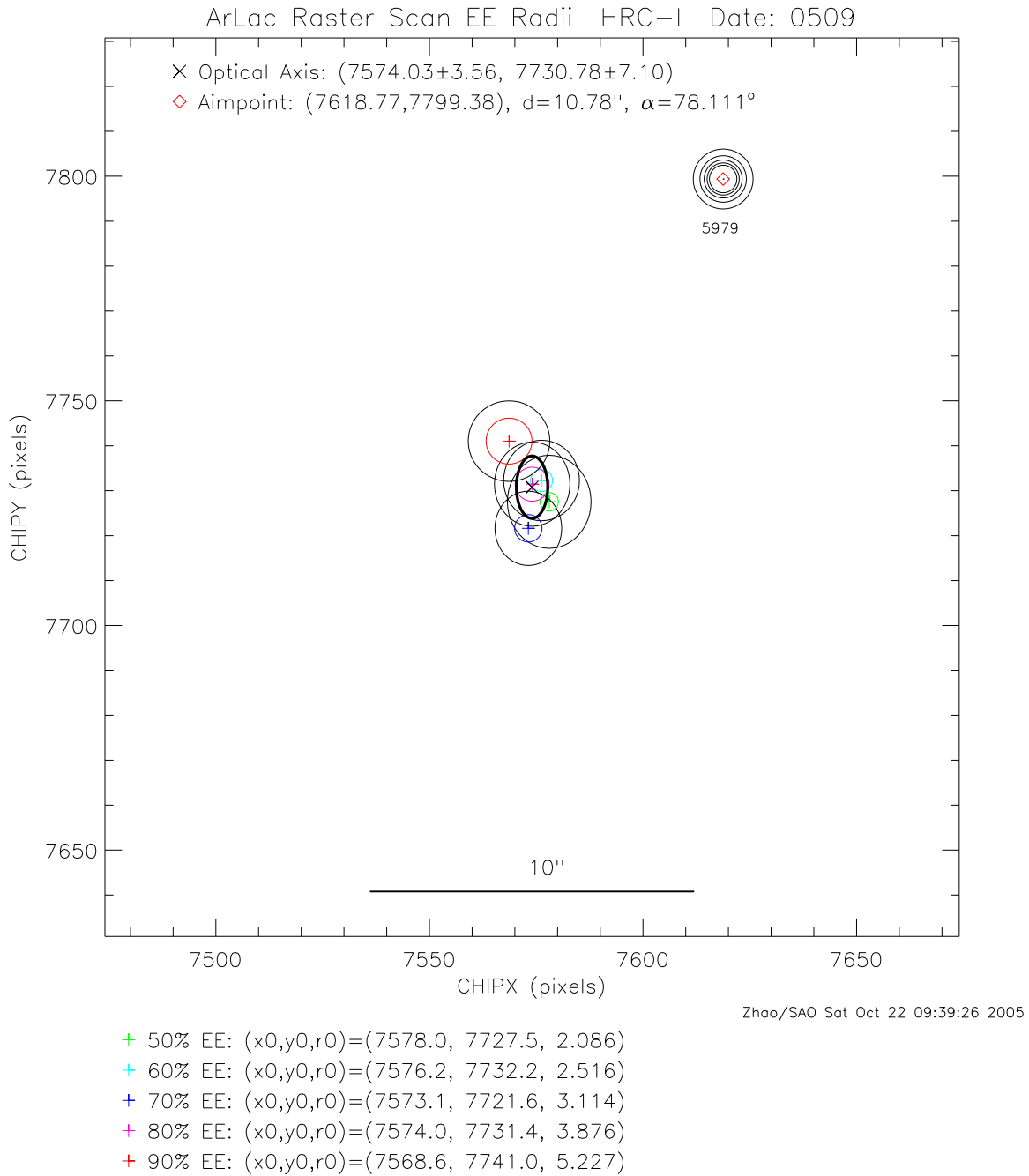Figure 7: Quadratic fit of HRC-I raster scan data of Ar Lac (Date: 2005-09-27).

Figure 8: Optical Axis and Aimpoint position on HRC-I, based on raster scan observation of Ar Lac made on 2005-09-27. The center × with the dark oval is the optical axis position and its error oval.

4   Results

The results of the Optical Axis and Aimpoint positions from all the raster scan data are summarized in Tables 3 and 4. The raster scan from 1999-09-02 on HRC-I was made near the upper corner of HRC-I at SIM-Z = 91.8655mm. The values in the table are transformed to SIM-Z=126.9855mm, using the clocking angle between the HRC-I u axis and the $-Z$ axis: $\theta = 44.704° \pm 0.003°$, instead of $45°$. This clocking angle value is based on the HRC-I alignment measurements made on 1999-09-02 with source HR1099, ObsIDs: 1211–1218, 1261 (see Figure 9). Michael Juda analyzed the same data and obtained a different clocking angle of $\theta = 44.87 \pm 0.01°$ (http://hea-www.harvard.edu/∼juda/memos/hrci_degap_lookup/capella/hrci_rotation.html). The difference between the two values could cause the transformed positions by 11 pixels in CHIPX and CHIPY. However, this difference has no effect for the rest of the analysis and the results, as the HRC-I optical axis was immediately measured again, only one month later, on 1999-10-03 at the center of the HRC-I. From then on, all the HRC-I raster scans were made at the center with the nominal SIM position (SIM-Z=126.9855mm, i.e. no transformation required). As shown in this table, the 1999-10-03 value is very close to the transformed 1999-09-02 value and well within their respective errors.

Table 3: Optical Axis and Aimpoints of HRC-I

Date of	Optical Axis (pixel)				Aimpoint (pixel)			
Raster Scan	CHIPX	error	CHIPY	error	CHIPX	error	CHIPY	error
1999-09-02*	7550.76	8.36	7725.72	11.54	7647.67	2.50	7671.18	1.86
1999-10-03	7553.90	10.31	7723.70	8.37	7646.57	4.40	7692.76	4.17
1999-12-09	7586.74	11.75	7746.42	6.30	7648.14	3.93	7710.21	4.60
2000-12-12	7582.96	15.06	7746.18	6.97	7648.68	4.05	7742.35	4.13
2002-01-26	7590.79	18.86	7740.97	4.16	7654.70	3.78	7758.74	4.03
2003-02-22	7604.43	13.52	7762.48	3.75	7664.35	3.73	7767.05	4.00
2004-11-25	7594.65	14.23	7740.04	9.02	7635.70	4.64	7784.81	4.48
2005-09-27	7574.03	3.57	7730.78	7.11	7638.84	8.62	7796.56	4.44

* This measurement was made near the upper corner of HRC-I at SIM-Z=91.8655mm (see text).

Table 4: Optical Axis and Aimpoints of HRC-S

Date of	Optical Axis (pixel)				Aimpoint (pixel)			
Raster Scan	CHIPX	error	CHIPY	error	CHIPX	error	CHIPY	error
2000-12-20	2300.12	16.42	8902.56	6.41	2153.29	2.74	8865.39	2.15
2001-05-14	2293.28	11.20	8907.65	9.93	2146.94	3.73	8868.29	1.68
2002-01-26	2283.63	14.37	8902.04	6.94	2136.85	3.00	8875.87	1.30
2002-08-09	2273.21	8.07	8886.97	4.34	2146.14	8.20	8871.43	1.11
2003-02-22	2273.60	15.94	8904.94	7.81	2126.35	5.64	8882.01	1.96
2003-09-01	2300.63	11.78	8915.85	9.96	2135.57	4.93	8903.12	2.20
2004-02-09	2271.17	4.21	8911.93	9.99	2111.21	2.92	8910.82	1.85
2004-11-28	2308.64	10.69	8904.08	8.55	2129.21	4.94	8907.23	1.62
2005-02-10	2262.44	8.23	8913.46	6.54	2118.35	9.24	8900.97	2.40
2005-09-01	2279.87	11.65	8904.08	9.16	2129.13	3.80	8912.34	2.18

Figures 10 and 11 illustrate the results in the HRC-I and HRC-S CHIP coordinates. The nominal positions are described in Section 1.

Figure 12 shows the position drifts of the optical axis and aimpoint on HRC-I during the first 6 years of Chandra operation. Figure 13 shows the position drifts of the optical axis and aimpoint, transformed from the HRC-I measurements to the HRC-S coordinate, using "*dmcoords*". As the figure shows, while the optical axis drift is more like random walk, the aimpoint is drifting consistently in the CHIPY (i.e. HRC-I v axis) direction. From Sept 1999 to Sept 2005, it drifted about 104 pixels, or 0.67mm, or $13.7''$.
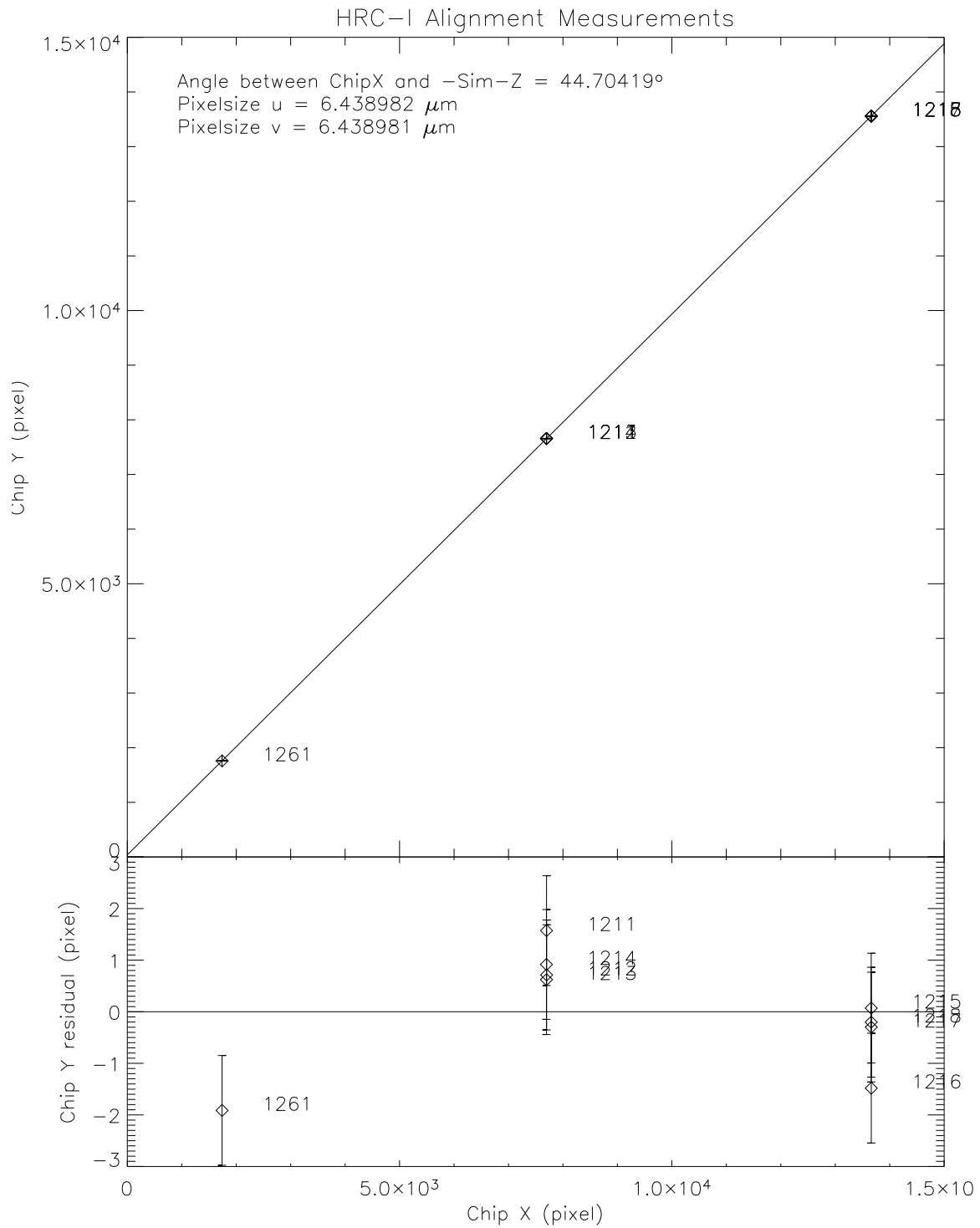
Figure 9: HRC-I alignment measurements (observations with dithering off): results show the clocking angle between +CHIPX and −Sim-Z is 44.70419°, instead of 45°.
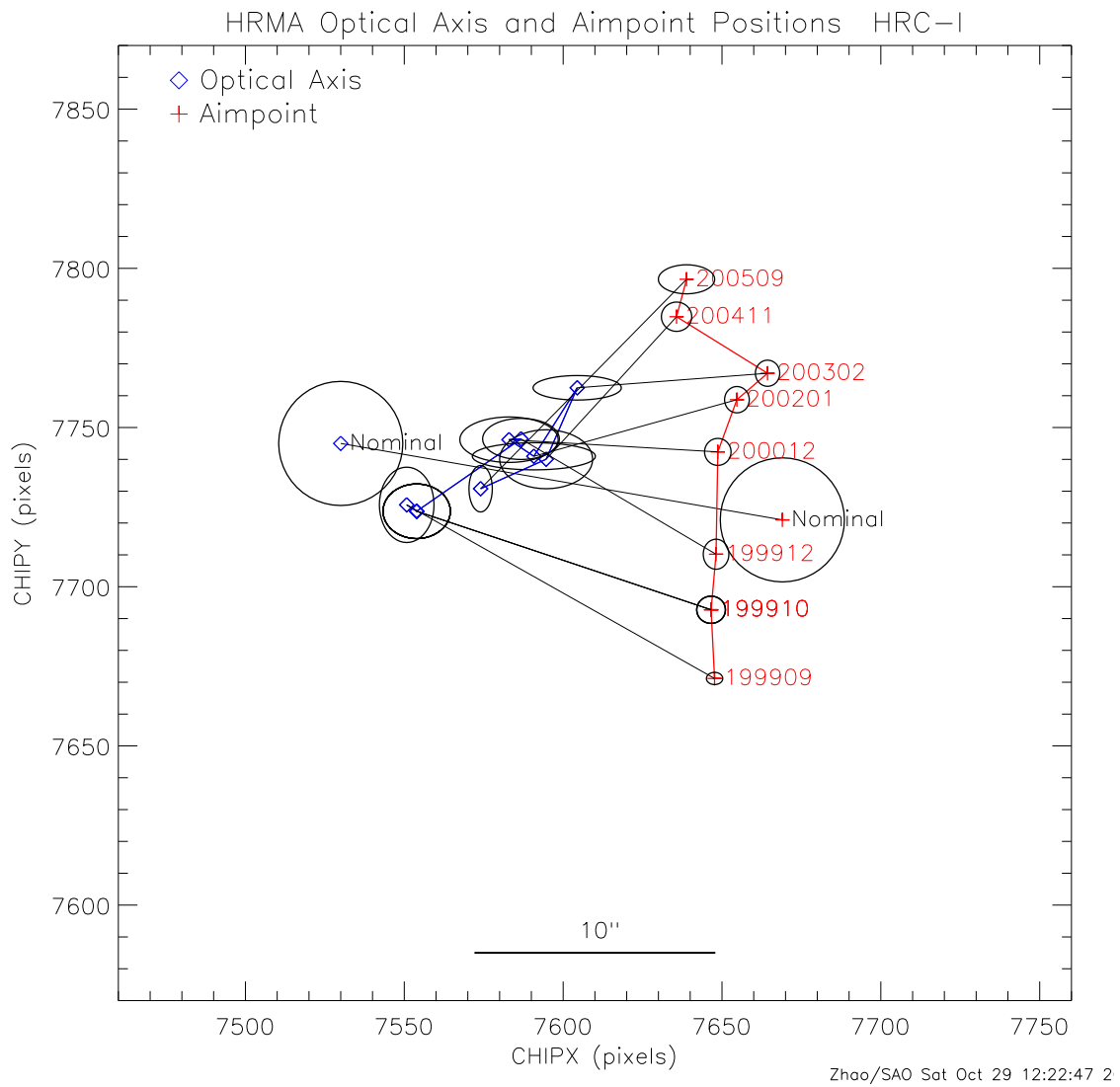
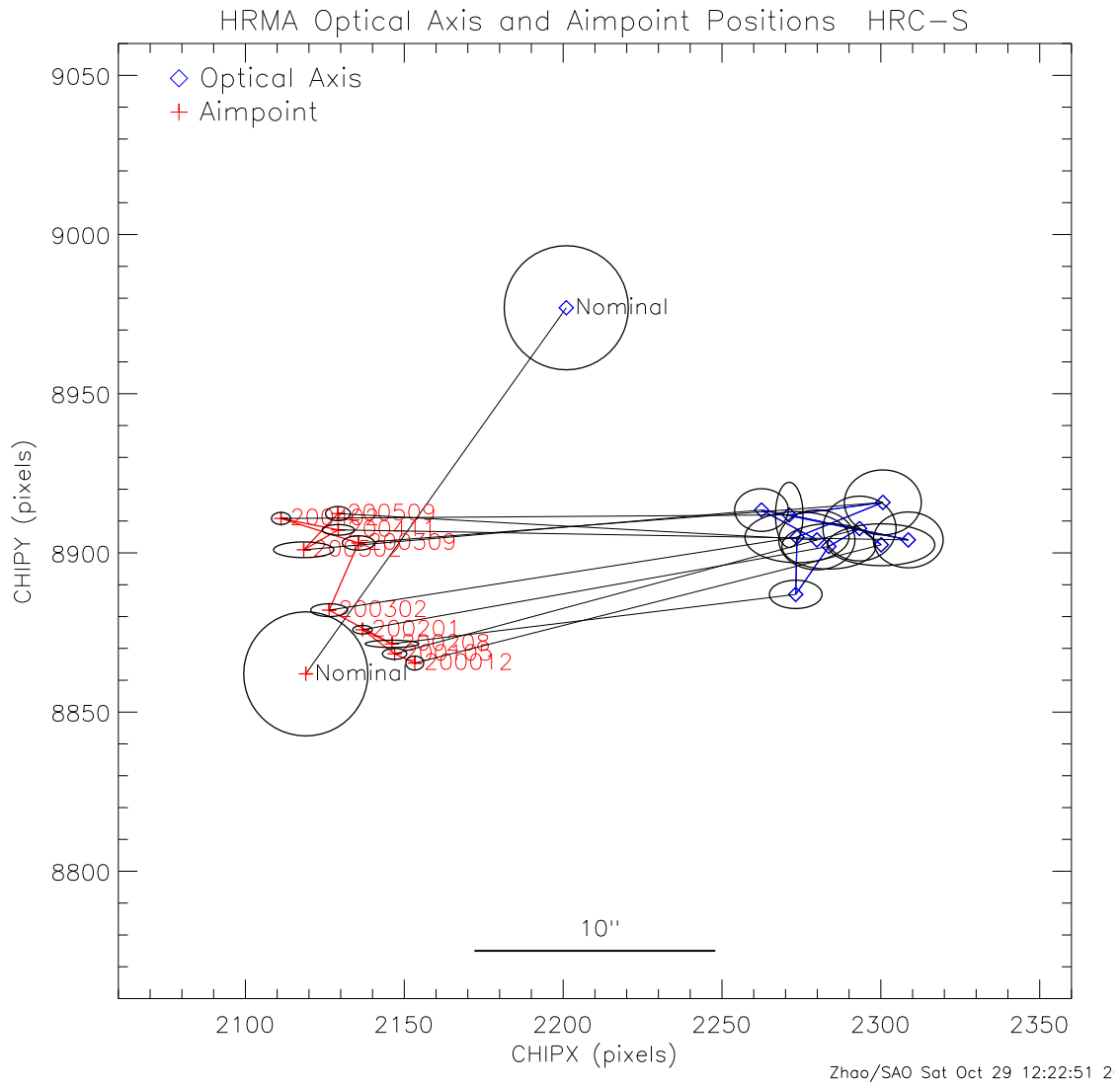Figure 10: Optical Axis and Aimpoint positions from all the HRC-I measurements on CHIP coordinates.

Figure 11: Optical Axis and Aimpoint positions from all the HRC-S measurements on CHIP coordinates.
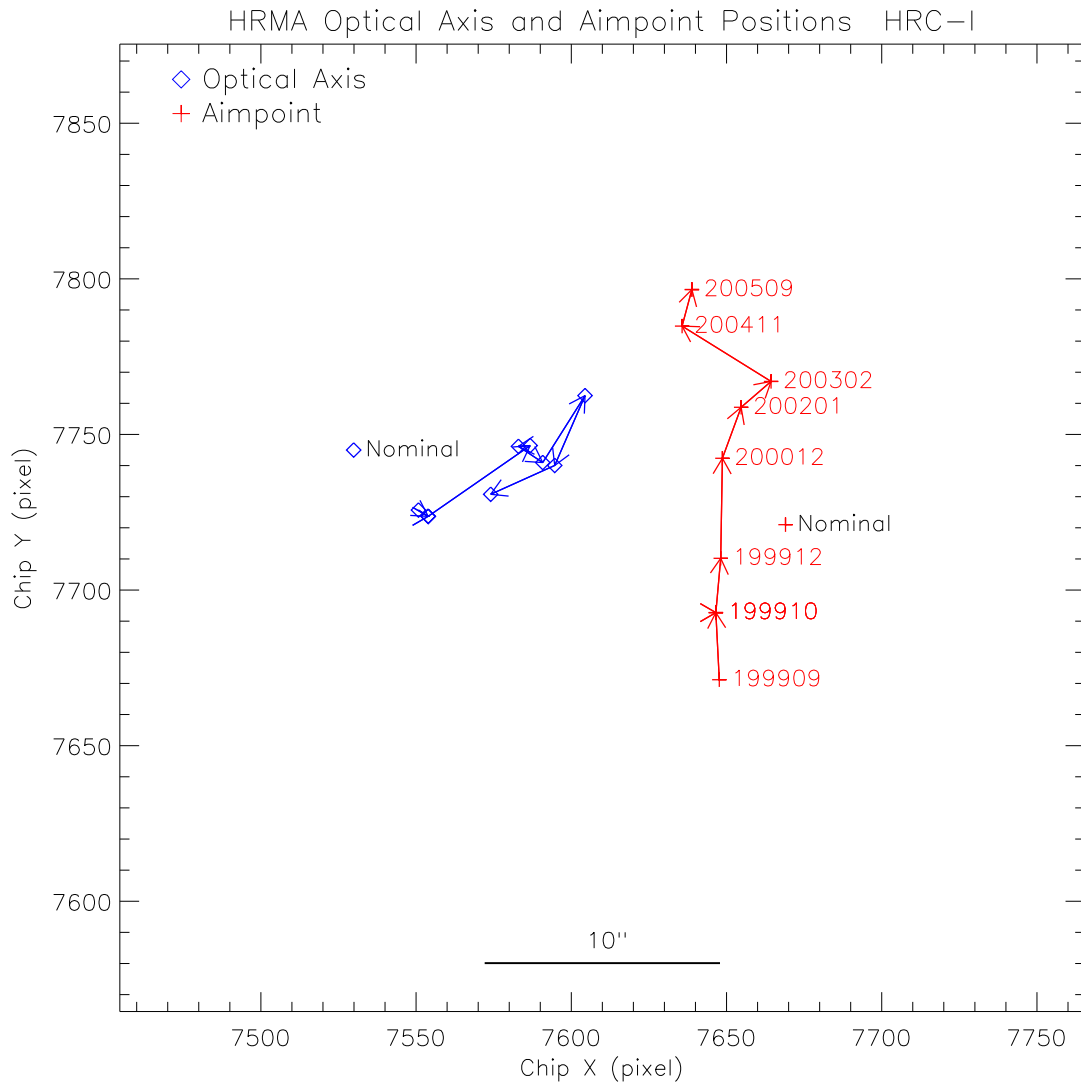
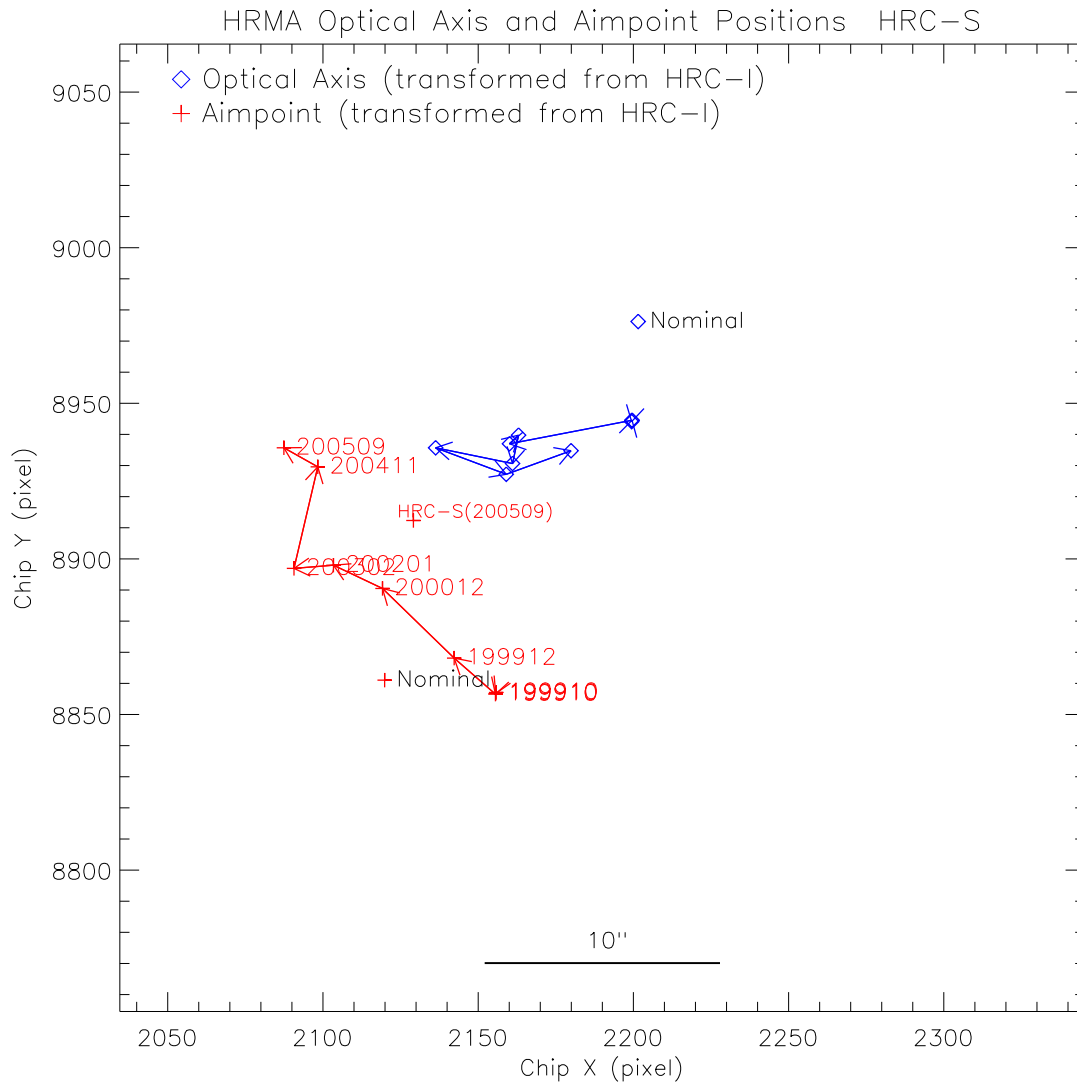Figure 12: Chandra Optical Axis and Aimpoint position drift on HRC-I.

Figure 13: Chandra Optical Axis and Aimpoint position drift on HRC-S, transformed from the HRC-I measurements.

5 Conclusion and its Impact on The Chandra Operation

Since the Chandra launch, its optical axis and aimpoint have been drifting continuously. The drift of the optical axis is like a random walk and within $10''$ range. The aimpoint has drifted in the HRC-I v axis direction for $\sim 13.7''$. The possible causes of these drifts include: 1) changes in the geometry of the spacecraft, such as a bending of the optical bench, causing the SIM module to shift with respect to the HRMA; 2) relative alignment between the aspect system and the telescope.

Now let's consider the possible impact of these drifts to the Chandra operation.

5.1 The separation between the optical axis and the aimpoint

Ideally, the optical axis and the aimpoint should be at the same location all the time. Thus the sources located at the aimpoint would have the sharpest PSF. The real HRMA is not ideal. The optical axis and the aimpoint were never at the same point and they are constantly drifting in different ways. However, their separation has always been within $15''$. Figures 14 and 15 are copies of page 46 and 47 from the Chandra Proposer's Observatory Guide, Rev.8.0, December 2005. They show the HRMA encircled energy on HRC-I and ACIS-I as a function of offaxis angle. As it is seen, a small offaxis angle of $15''$ (from the optical axis) causes no degradation on the encircled energy, hence also no degradation on the PSF.

5.2 The optical axis and the aimpoint positions on the Detectors

Since the positions of the optical axis and the aimpoint have been drifting, we need to re-examine their positions on each detector to ensure they are not falling off the boundary of the detector or node.

Figures 12 and 13 have shown that the optical axis and the aimpoint positions are always near the centers of the HRC-I and HRC-S (see the CHIP coordinate). So the dither pattern (amplitude is $40''$ peak-to-peak, POG Rev.8 p73) is well within the detector boundary.

Figure 16 is a copy of page 78 from the Chandra Proposer's Observatory Guide, Rev.8.0, December 2005. It shows the ACIS detector layout and the nominal aimpoint positions on the ACIS-I3 and ACIS-S3 chips.

Figure 17 shows the optical axis and the aimpoint positions on ACIS-I3. They are near the inner corner of I3, but still well within the detector boundary.

Figure 18 shows the optical axis and the aimpoint positions on ACIS-S3. In 1999, the aimpoint is very close to the boundary of node 0 and 1. In order to keep the target source dither pattern ($16'$ peak to peak) entirely within one node, it was decided that, for default operation, the target will have $Y - offset = -20''$. However, as illustrated in Figure 18, the aimpoint has drifted towards the $+$Y-offset direction. A $-20''$ offset would make part of the dither pattern fall into the node boundary. Thus, a decision was made to change the default Y-offset from $-20''$ to $+10''$ to avoid the node boundary. This decision was announced in Chandra Electronic Bulletin No. 43:

"NEW DEFAULT TARGET OFFSETS for ACIS-S

The CXC recommends a revised target pointing offset for ACIS-S observations to place the target closest to the aimpoint while avoiding a node boundary. The default Y-offset value for ACIS-S target is henceforth changed from -0.33 arcmin (-20 arcsec) to +0.17 arcmin (+10 arcsec). The new recommended +0.17 arcmin Y-offset will be used for all approved ACIS-S targets that are unobserved as of Oct 9, 2005 and that either explicitly or by default had a Y-offset value of -0.33 arcmin in their proposals.

Table 5 summarizes all the positions of the optical axis and aimpoint.

Chapter 4. High Resolution Mirror Assembly (HRMA)

Figure 4.12: HRMA/HRC-I encircled energy average radii for circles enclosing 50% and 90% of the power at 1.49 and 6.40 keV as a function of off-axis angle. The HRC-I surface is a flat plane perpendicular to the optical axis, which does not follow the curved *Chandra* focal plane. These curves include the blurs due to the HRC-I spatial resolution and the *Chandra* aspect error.

Figure 14: Page 46 of Chandra Proposer's Observatory Guide, Rev.8.0, December 2005
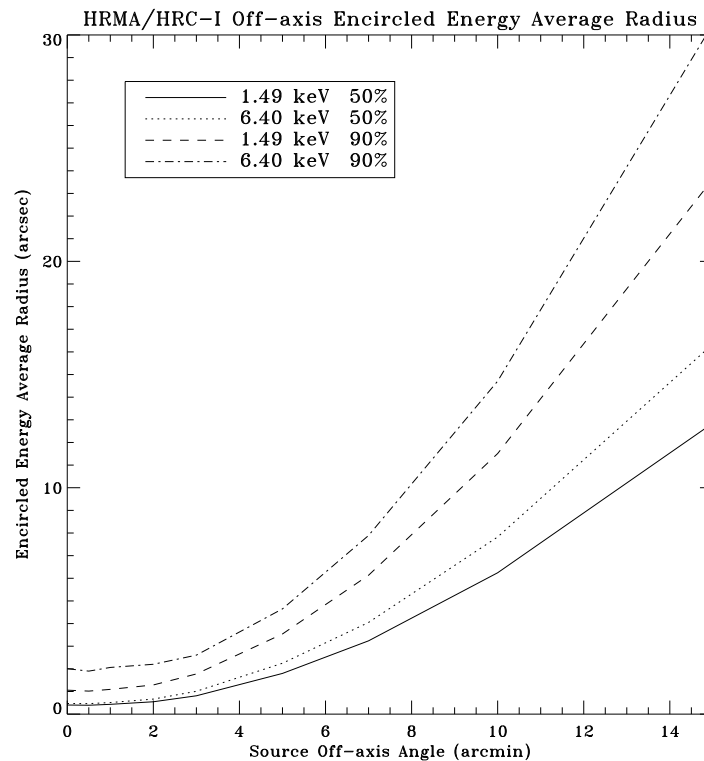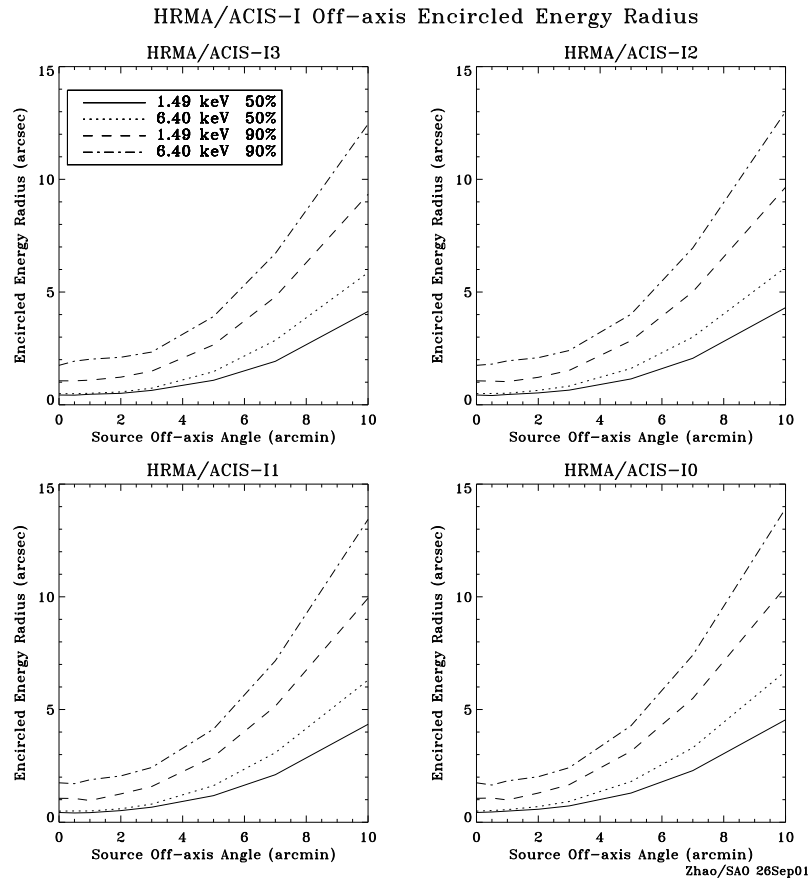
4.2. Calibration and Performance

Figure 4.13: HRMA/ACIS-I encircled energy radii for circles enclosing 50% and 90% of the power at 1.49 and 6.40 keV as a function of off-axis angle. The ACIS-I surface is composed by four tilted flat chips which approximate the curved *Chandra* focal plane. The HRMA optical axis passes near the aimpoint which is located near the inner corner of chip I3. Thus the off-axis encircled energy radii are not azimuthally symmetric. The four panels show these radii's radial dependence in four azimuthal directions – from the aimpoint to the outer corners of the four ACIS-I chips. These curves include the blurs due to the ACIS-I spatial resolution and the *Chandra* aspect error.

Figure 15: Page 47 of Chandra Proposer's Observatory Guide, Rev.8.0, December 2005

ACIS FLIGHT FOCAL PLANE

~22 pixels ~11" →   ← **not** constant with Z

I0	I1
w203c4r	w193c2
0	1

22 pixels = 11"

I2	x I3
w158c4r	w215c2r
2	3

} ACIS-I

(aimpoint on I3 = (949, 978))

330 pixels = 163"

S0	S1	S2	S3 +	S4	S5
w168c4r	w140c4r	w182c4r	w134c4r	w457c4	w201c3r
4	5	6	7	8	9

} ACIS-S

(aimpoint on S3 = (235, 497))

18 pixels = 8".8

BI chip indicator →

Image Region

Pixel (0,0)

Frame Store

Top

Bottom

CCD Key

node zero / one / two / three

Node Definitions

row / column

Row/Column Definition

+ Δ Y   **Target**
Offset Coordinates

+Z   +Z

Pointing Coordinates

+ Δ Z

-Z

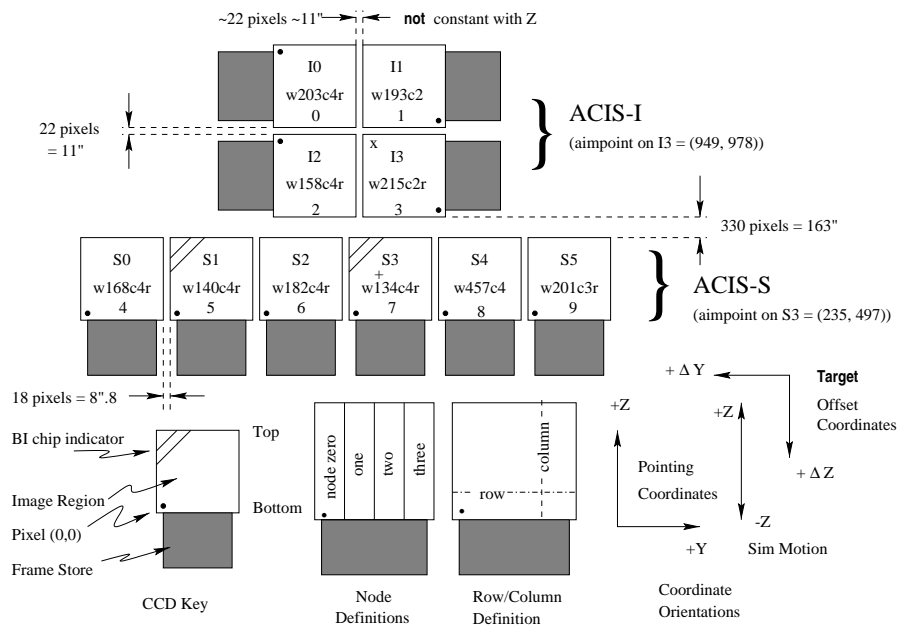+Y   Sim Motion

Coordinate Orientations

Figure 6.1: A schematic drawing of the ACIS focal plane; insight to the terminology is given in the lower left. Note the nominal aimpoints: on S3 (the '+') and on I3 (the 'x'). It is standard practice to add an offset to all observations on S3 to move the source away from the node 0-1 boundary (see Section 6.9) Note the differences in the orientation of the I and S chips, important when using Subarrays (Section 6.11.3). Note also the (Y, Z) coordinate system and the target offset convention (see Chapter 3) as well as the SIM motion (+/-Z). The view is along the optical axis, from the source toward the detectors, (-X). The numerous ways to refer to a particular CCD are indicated: chip letter+number, chip serial number, and ACIS chip number. The node numbering scheme is illustrated lower center.

Figure 16: Page 78 of Chandra Proposer's Observatory Guide, Rev.8.0, December 2005
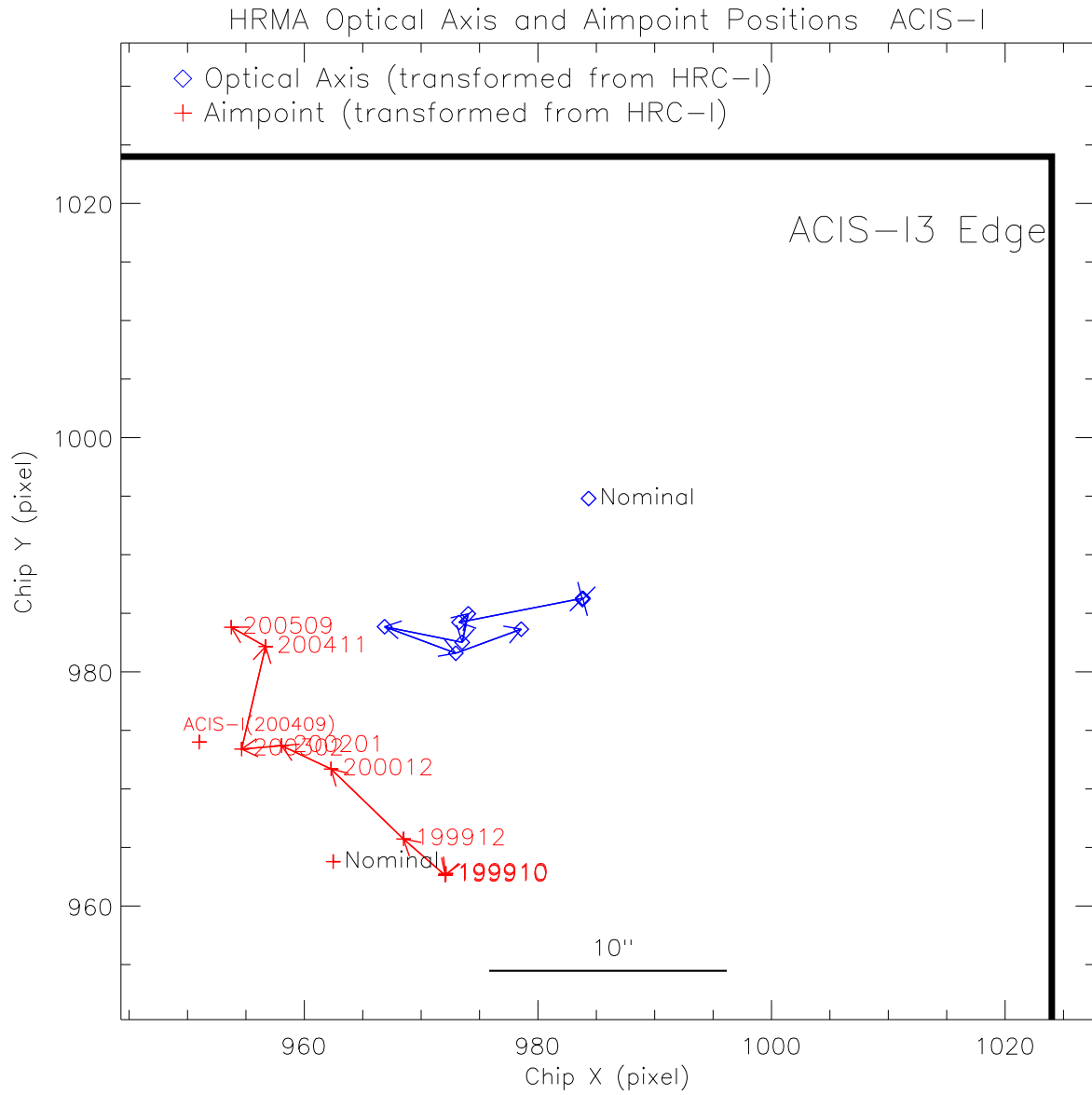
Figure 17: Chandra Optical Axis and Aimpoint positions on ACIS-I, transformed from the HRC-I measurements. (Node boundary is outside of the figure.)
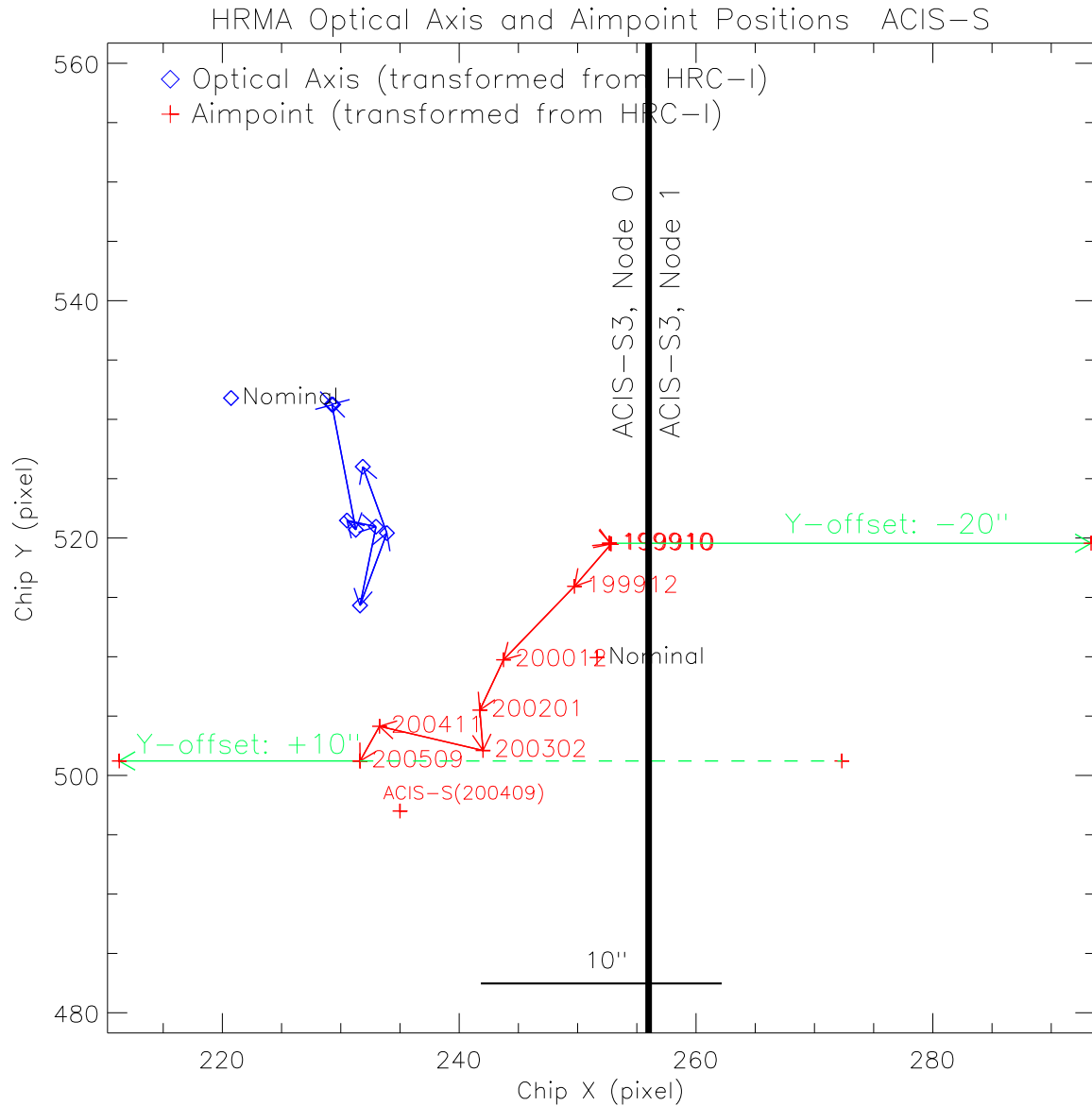
Figure 18: Chandra Optical Axis and Aimpoint positions on ACIS-S, transformed from the HRC-I measurements. Because of the aimpoint drift, the default target pointing offset for ACIS-S observations has been changed from Y-offset=$-20''$ to Y-offset=$+10''$ to avoid the node boundary during dither ($16''$ peak to peak), as announced in Chandra Electronic Bulletin No. 43. This change also puts the target pointing closer to the Optical Axis.

Table 5: Optical Axis and Aimpoint Positions

Detector	SIM-Z (mm)	Point	Nominal[a] CHIPX	CHIPY	Actual[b] CHIPX	CHIPY	Current[c] CHIPX	CHIPY	Current(HRC-I)[d] CHIPX	CHIPY
HRC−I	126.985	opax	7529.90	7745.00	7551.08	7725.13	7574.03	7730.78	7574.03	7730.78
		aimp	7669.00	7721.00	7669.00	7721.00	7638.84	7796.56	7638.84	7796.56
HRC−S	250.456	opax	2201.53	8976.27	2200.42	8947.27	2279.87	8904.08	2179.91	8934.76
		aimp	2119.88	8861.03	2119.88	8861.03	2129.13	8912.34	2087.42	8935.69
ACIS−I	−233.592	opax	984.34	994.80	984.05	987.02	—	—	978.57	983.64
		aimp	962.47	963.79	962.47	963.79	951.00	974.00	953.75	983.80
ACIS−S	−190.133	opax	220.73	531.80	228.51	531.50	—	—	231.86	526.01
$\Delta Y=0''$		aimp	251.64	509.93	251.64	509.93	235.00	497.00	231.63	501.22
$-20''$		aimp	292.32	509.93	—	—	275.68	497.00	272.31	501.22
$+10''$		aimp	231.30	509.93	—	—	214.66	497.00	211.29	501.22

[a] Nominal (default) positions based on measurements made in September 1999, on HRC-I (optical axis) and ACIS-S (aimpoint). These are the numbers in the Calibration Database and POG since 1999.

[b] Actual optical axis positions based on the same measurements but taking into account of the HRC-I clocking angle — the angle between +CHIPX and −Sim-Z is 44.70419°, instead of 45°. The aimpoints are the same as Nominal.

[c] Current optical axis and aimpoint positions, based on measurements made in September 2005 for HRC-I and HRC-S, and in September 2004 for ACIS-I and ACIS-S.

[d] Current optical axis and aimpoint positions, based on measurements made in September 2005 for HRC-I and translated onto other detectors using the *dmcoords* and the current *geom* file in the Calibration Database.